Theor Chem Account (2008) 120:295–305
DOI 10.1007/s00214-007-0313-7

REGULAR ARTICLE

Intrinsic local constituents of molecular electronic wave functions. II. Electronic structure analyses in terms of intrinsic oriented quasi-atomic molecular orbitals for the molecules FOOH, $H_2BH_2BH_2$, H_2CO and the isomerization HNO → NOH

Joseph Ivanic · Klaus Ruedenberg

Received: 9 January 2007 / Accepted: 12 February 2007 / Published online: 22 May 2007

Abstract The electronic bonding structures of the molecules FOOH, H_2CO, $H_2BH_2BH_2$ and the isomerization HNO → NOH are analyzed in terms of the intrinsic, oriented quasi-atomic molecular orbitals that are extracted from the optimized full-valence multi-configuration self-consistent-field wavefunctions by the unbiased, basis-set-independent procedure described in the preceding paper. In all cases, the method brings to light the essentials of the bonding interactions. Detailed insights are furnished regarding the hyperconjugation between lone pairs and nearby antibonding orbitals in FOOH and H_2CO, regarding the three-center bonding in diborane, and regarding the transition state structure in HNO. The versatility of the use of the quasi-atomic orbitals is exemplified.

1 Introduction

The objective of the analysis in the preceding study [1] was to cast accurate ab-initio molecular electronic wavefunctions into forms revealing that they are predominantly built from atomic components. It was noted that the zeroth-order approximations to such wavefunctions can typically be expressed as multiconfiguration self-consistent-field (MCSCF) wavefunctions *in full valence spaces*, and the proposition was advanced that such full valence space functions can typically be represented as superpositions of configurations that are generated from molecular orbitals having *quasi-atomic* character, i.e. differing from corresponding free-atom orbitals only by slight deformations.

Practical methods were developed for localizing the molecular orbitals (MOs) of accurate full-valence-space wavefunctions as strongly as possible. Notably, a new method was developed for orienting ("hybridizing") quasi-atomic MOs that would exhibit bonding interactions as lucidly as possible. We called these methods *"intrinsic"* because:

- The quasi-atomic nature as well as the directional properties of the orbitals are extracted from the *exact* density by an *unbiased* formalism, which is *basis-set-independent* and *does not take account of any preconceived information* such as, e.g., regarding the location of two-center or multi-center bonds.
- Although the quasi-atomic orbitals are of the minimal-basis-set type, they are in fact molecular orbitals and the accurate full-valence-space wavefunction can be *exactly* recovered as a superposition of the determinants generated from these orbitals.

By casting a molecular electronic wavefunction in this form one obtains what we have called its *Intrinsic Localized Density Analysis (ILDA)*.

The results to be reported in the present study demonstrate that the ILDA method does in fact achieve the desired goal. Applications to four systems will illustrate how this approach can be used to gain insights into various aspects of electronic structure and bonding, and opens quantum mechanical ab-initio results up to chemical interpretations.

In order to clearly emphasize the intrinsic nature of the present approach, we here choose the quasi-atomic orbitals

Contribution to the Mark S. Gordon 65th Birthday Festschrift Issue.

J. Ivanic · K. Ruedenberg (✉)
Ames Laboratory USDOE and Department of Chemistry,
Iowa State University, Ames, IA 50011, USA
e-mail: ruedenberg@iastate.edu

Present Address:
J. Ivanic
Biotechnology HPC Software Applications Institute,
US Army Medical Research and Materiel Command,
Ft. Detrick, MD 21702, USA

to be the orbitals that result straight from an intrinsic localization procedure, i.e. their atomic localization is not further enhanced by atomic adaptations of the kind discussed in Sect. 4.2 of Ref. [1]. For each molecule, we obtain the full-valence-space MCSCF wavefunction, which we have called its FORS (full optimized reaction space) wavefunction [2–5]. We then localize the FORS MOs by the Edmiston-Ruedenberg procedure (See Sect. 3.2 of the proceeding paper), mixing all valence orbitals and all core orbitals regardless of their irreducible representations, so as to achieve the highest degree of localization. Since, in each case, the localized orbitals turn out to be strongly quasi-atomic, the novel orientation procedure developed in Sect. 7 of the preceding paper [1] is then applied.

Inferences regarding the bonding interactions are drawn from the orbital populations and bond orders, i.e. the diagonal and off-diagonal elements of the density matrices generated by these *intrinsic oriented quasi-atomic MOs*, in conjunction with plots displaying them. From the latter, one can infer the orbital directions, the s–p mixing and usually the sign of orbital overlaps. (We leave the quantitative examination of the inherent s–p mixings, i.e. the "hybridizations", to future discussions.) Bonding is to be expected if a bond order has the same sign as the corresponding overlap integral. It furthermore transpires that elucidating insights into molecular bonding structures emerge from considering not only the quasi-atomic orbitals but also the split-localized MOs, which were introduced in Sect. 3.1 of Ref. [1], as well as "reduced" split-localized orbitals, expressed in terms of the quasi-atomic orbitals.

All wavefunctions were calculated using Dunning's cc-pVTZ basis sets [6], except that *d* functions were removed from the H atoms and *f* functions were removed from the other atoms. The MCSCF calculations were performed using a previously described direct full configuration interaction (FCI) code [7] coupled with the near-second-order orbital optimization method of Chaban, Schmidt, and Gordon [8]. The displayed orbital plots correspond to the contour surfaces for $0.1\,\mathrm{bohr}^{-3/2}$, which is the default value of the plotting program. In these pictures, the small tails of the quasi-atomic orbitals do not always show up, but they are of course there, ensuring the mutual orthogonalities. The GAMESS program system [9] was used for all procedures.

2 Bonds and lone pairs in FOOH

The FOOH molecule has several bonds as well as lone pairs on different atoms. It therefore presents a good starting point for testing the ability of our procedure to generate quasi-atomic orbitals that separate the two types effectively.

The molecule belongs to the point group C_1 so that the first order density matrix is not simplified due to symmetry. Since there is no experimental geometry for FOOH, we used the optimized structure of T. Lee et al. [10] with the structural parameters: $r_{FO} = 1.481$ Å, $r_{OO} = 1.393$ Å, $r_{OH} = 0.969$ Å, $\angle_{FOO} = 105.4°$, $\angle_{OOH} = 101.9°$, $\tau_{FOOH} = 84.5°$. This structure seems reliable because, for FOOF, the same authors obtain a structure very close to the experimental one. The full configuration space for the ground state contains 81,796 determinants. We obtained the SCF energy −249.58973 hartree and the FORS energy −249.74492 hartree.

The oriented quasi-atomic orbitals are displayed in Fig. 1. The atoms are, from left to right: F, O, O*, H. The label Fℓ denotes a lone pair orbital on F, the label Fo denotes an orbital on F pointing toward O, the label Of denotes an orbital O pointing toward F, and so on. The elements of the density matrix in this orbital basis are displayed in Table 1.

The occupation numbers in the bold boxes on the diagonal of the matrix are also entered next to the orbital symbols on the figure. Summing them on each atom yields the total valence electronic charges 7.10, 5.98, 5.98, and 0.94 on the quasi-atoms F, O, O*, and H, respectively, reflecting the relative electronegativities of these atoms.

All matrix elements are rounded to two decimal places and no entry is made when the value is less than 0.01. This is manifestly the case for most of the bond orders, i.e. the off-diagonal elements. In addition, the bulk of the remaining bond orders are also very small. Only the three boldfaced bond orders are large, namely those corresponding to the bonds Fo–Of, Oo–Oo* and Oh–H, having the values 0.84, 0.93 and 0.97, respectively. They are also entered on Fig. 1 between arrows pointing to the orbitals involved. These clearly have the appearance of sigma bonding quasi-AOs which, in the case of Fo, Of, Oo, Oo* and Oh*, point towards the bonded orbital on the neighboring atom. All of them have occupations (diagonal elements) close to one.

The remaining seven orbitals have occupations close to two, small bond orders and spatial appearances that clearly identify them as lone pairs.

The density matrix reveals however an additional bonding feature, namely the weak but not negligibly small bond orders of 0.28 and −0.24 between the lone pair orbital Oℓ2* and the bonding orbitals Of and Fo, respectively. These three orbitals all lie in the FOO* plane. Correspondingly, the occupation of Oℓ2* is only 1.91, markedly lower than that of the other lone pair orbitals. The reasons become clear when we examine, in addition to the quasi-atomic representation, also a *"local split-localized"* presentation (see Sect. 3.1. of Ref. [1]): In the present case, the bonding and anti-bonding *molecular* orbitals, labeled OFb and OFa, between the quasi-atomic orbitals Of and Fo are formed by diagonalizing the corresponding 2×2 density sub-matrix. These orbitals are manifestly closely related to the split-localized orbitals discussed in Sect. 3.1 of the preceding paper [1]. The density matrix between these two *molecular* orbitals and the

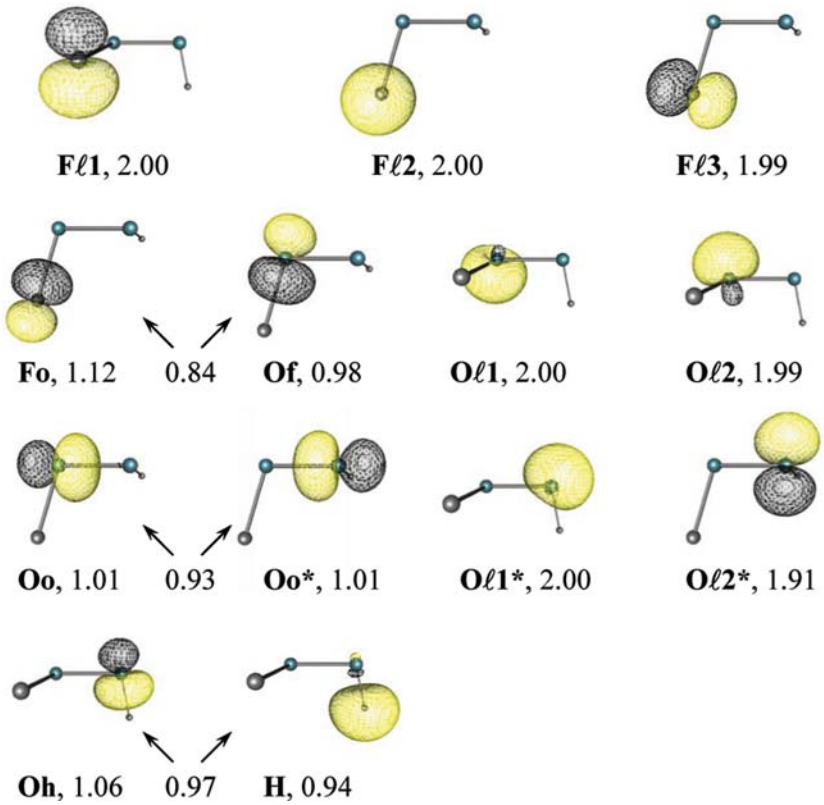

Fig. 1 Oriented quasi-atomic orbitals for FOOH. The occupation numbers are given next to the orbital labels and large bond orders are indicated between *arrows* pointing to the orbitals involved

Table 1 Density matrix for FOOH after localization and after orientation

QAO	Fℓ1	Fℓ2	Fℓ3	Fo	Oℓ1	Oℓ2	Oo	Of	Oℓ1*	Oℓ2*	Oh*	Oo*	H
Fℓ1	**2.00**										−0.01		0.01
Fℓ2		**2.00**		−0.02									
Fℓ3			**1.99**				0.11				−0.01	−0.10	0.02
Fo		−0.02		**1.12**				**0.84**		−0.24		0.07	
Oℓ1					**1.99**			−0.02					
Oℓ2						**1.99**		−0.02			−0.03		0.03
Oo			0.11				**1.01**	−0.08				**0.93**	−0.05
Of				**0.84**	−0.02	−0.02	−0.08	**0.98**		0.28			
Oℓ1*									**2.00**			0.01	
Oℓ2*				−0.24				0.28		**1.91**		0.03	
Oh*	−0.01		−0.01			−0.03					**1.06**	0.05	**0.97**
Oo*			0.10	0.07			**0.93**		0.01	0.03	0.05	**1.01**	
H	0.01		0.02			0.03	−0.05				**0.97**		**0.94**

lone pair orbital Oℓ2* is displayed in Table 2. It is apparent that a slight bonding interaction exists between Oℓ2* and the anti-bonding OFa molecular orbital. Thus, there is a tendency to establish some π bonding between O* and O, but this can be had only by using the anti-bonding OFa molecular orbital since the corresponding bonding OFb orbital has an occupation close to two. Consequently, the bond order with the Fo quasi-atomic orbital is negative, but the corresponding energy integral is presumably smaller than that between Oℓ2* and the closer Of orbital. Such an incipient dative bonding between a lone pair and a weakly occupied anti-bonding MO nearby has been called hyperconjugation. It can thus be attributed to a partial pi-bond formation between oxygen and carbon *combined with the correlation stabilization furnished by the OFa orbital for the OFb bonding orbital*.

In order to exhibit the importance of *the transformation to oriented quasi-atomic orbitals*, we also show the density matrix for the localized quasi-atomic orbitals *before* this

Table 2 Density matrix for OF bonding and anti-bonding orbitals with Oℓ2*

MO	OF_b	OF_a	Oℓ2*
OF_b	**1.90**		0.01
OF_a		**0.20**	0.37
Oℓ2*	0.01	0.37	**1.91**

transformation was performed. It is shown in Table 3 where, as in Table 1, the elements are rounded off to two decimals and only elements with values 0.01 or larger are listed. The great simplifications accomplished by the orientation transformation yielding Table 1 are manifest.

3 Bonding structure changes along the reaction path HNO → NOH

While concepts pertaining to electronic structures of stable molecular ground states are well developed, more uncertainty regarding such structures exists for systems in transition states, where more complex electronic arrangements can be expected. In order to test what our approach can contribute in such situations, we analyze the transition state on the hydrogen transfer reaction path along which HNO converts to NOH.

The two minima as well as the transition state lie on the $1^1A'$ potential energy surface of the C_s point group. The geometries of all three critical points were optimized. The structures are given in Table 4 together with the experimental structure of HNO [11]. The number of determinants in this symmetry is 3,528. The SCF energies obtained for HNO, NHO*, NOH are −129.83001, −129.69437, −129.77868 hartree, respectively; the corresponding FORS energies are −129.96779, −129.85114, and −129.89863 hartree.

The oriented quasi-atomic orbitals are illustrated in Fig. 2. Each *column* corresponds to one *critical point* as indicated by the picture at the top. The *first three rows* contain the three *oriented quasi-atomic orbitals* on nitrogen, hydrogen and oxygen, respectively, that are *essentially involved in the electronic rearrangement* when the bonding shifts from being between N and H, to being between O and H, with all three atoms being somewhat bonded at the transition state. Rows 4 and 5 display the quasi-atomic orbitals on nitrogen and oxygen, respectively, that form the NO sigma-bond. Rows 6 and 7 display the quasi-atomic orbitals on nitrogen and oxygen, respectively, that form the NO pi-bond. The last two rows display the persistent lone pair orbitals on nitrogen and oxygen, respectively.

The corresponding density matrices for the three critical points are given in Tables 5, 6, and 7, respectively. All elements with a value less than 0.01 are omitted, which reveals that there are only few essential interactions, which are indi-

Table 3 Density matrix for FOOH after localization and before orientation

QAO	F1	F2	F3	F4	O1	O2	O3	O4	O1*	O2*	O3*	O4*	H
F1	**1.48**	0.23	−0.23	0.29	−0.25	−0.12	−0.46	0.34	0.02	−0.08	−0.06	0.16	
F2	0.23	**1.89**	0.10	−0.13	0.09	0.05	0.24	−0.14	−0.04	0.06	0.01	−0.08	0.02
F3	−0.23	0.10	**1.89**	0.12	−0.18	−0.06	−0.15	0.20	−0.02	0.03	−0.07	0.06	0.02
F4	0.29	−0.13	0.12	**1.84**	0.12	0.06	0.29	−0.18	−0.02	0.08	0.02	−0.09	
O1	−0.25	0.09	−0.18	0.12	**1.42**	−0.15	0.12	0.50	−0.17	0.46	−0.33	0.04	0.04
O2	−0.12	0.05	−0.06	0.06	−0.15	**1.94**	−0.08	0.16		0.07	−0.07	0.04	−0.02
O3	−0.46	0.24	−0.15	0.29	0.12	−0.08	**1.12**	0.14	0.18	−0.55	0.20	0.22	−0.24
O4	0.34	−0.14	0.20	−0.18	0.50	0.16	0.14	**1.50**	0.10	−0.28	0.26	−0.10	−0.02
O1*	0.02	−0.04	−0.02	−0.02	−0.17		0.18	0.10	**1.09**	−0.06	−0.04	−0.04	0.93
O2*	−0.08	0.06	0.03	0.08	0.46	0.07	−0.55	−0.28	−0.06	**1.22**	0.41	0.10	0.28
O3*	−0.06	0.01	−0.07	0.02	−0.33	−0.07	0.20	0.26	−0.04	0.41	**1.74**	−0.01	−0.07
O4*	0.16	−0.08	0.06	−0.09	0.04	0.04	0.22	−0.10	−0.04	0.10	−0.01	**1.92**	0.01
H		0.02	0.02		0.04	−0.02	−0.24	−0.02	0.93	0.28	−0.07	0.01	**0.94**

Table 4 Geometric parameters of HNO, NHO* and NOH

HNO	HNO(Exp)[9]	NHO*	NOH
$r_{HN} = 1.076$ Å	$r_{HN} = 1.063$ Å	$r_{HN} = 1.277$ Å	$r_{HO} = 0.993$ Å
$r_{NO} = 1.215$ Å	$r_{NO} = 1.212$ Å	$r_{NO} = 1.357$ Å	$r_{NO} = 1.278$ Å
$\angle_{HNO} = 108.7°$	$\angle_{HNO} = 108.6°$	$\angle_{HNO} = 49.5°$	$\angle_{HON} = 108.8°$

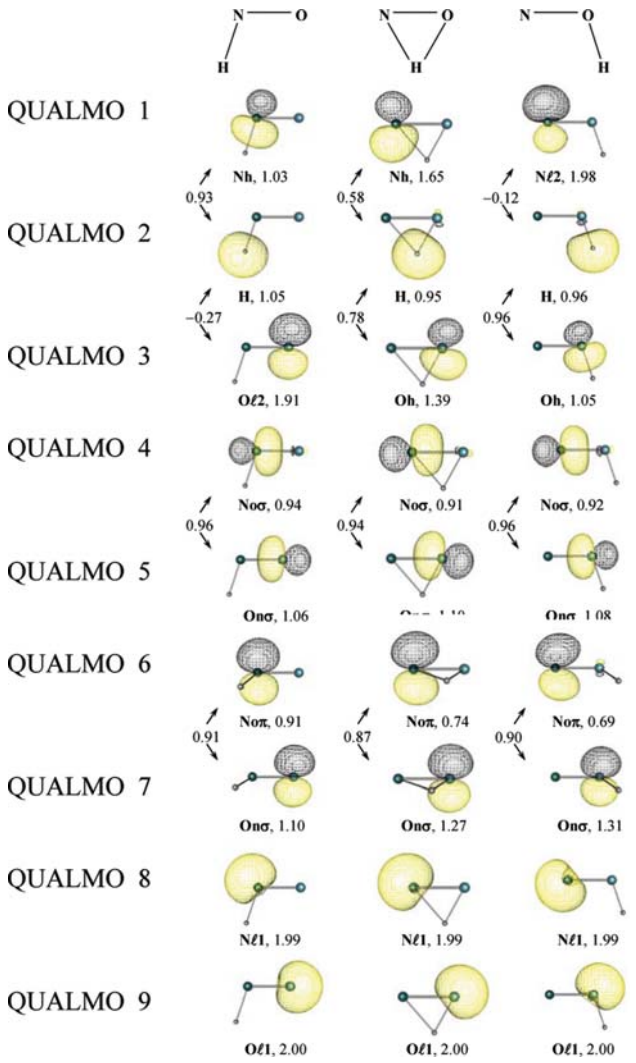

Fig. 2 Oriented quasi-atomic orbitals for HNO, NHO* and NOH. In accordance with Sect. 4.1 of Ref. [1], they are denoted as QUALMOs. Occupation numbers are given next to the orbital labels and large bond orders are indicated between *arrows* pointing to the orbitals involved

cated by boldfaced bond orders. The occupation numbers and the significant bond orders are also entered on the figure in the same way as was done for FOOH.

It is apparent that the quantities referring to all of the orbitals in the *last six* rows change very little during the isomerization. The NO sigma and pi bonding orbitals, one lone-pair orbital on N and one lone-pair orbital on O therefore have the character of spectator orbitals during the isomerization. These lone pair orbitals are deformed 2s atomic orbitals, as can be seen from their shapes.

All electronic rearrangements occur between the orbitals in first three rows of Fig. 2. As the hydrogen moves from nitrogen to oxygen, its orbital occupation remains close to unity. In HNO it is bonded to the Nh orbital (bond order 0.93); in NOH it is bonded to Oh (bond order 0.96). Along the reaction path, the bonding orbital Nh with population 1.03 in HNO changes into the lone pair orbital Nℓ2 with population 1.98 in NOH. At the transition state, its population is 1.65. Correspondingly, the lone pair orbital Oℓ2 with population 1.91 in HNO changes into the bonding orbital Oh with population 1.05 in NOH. At the transition state, its population is 1.39. For all three geometries, the sum of the populations of these three orbitals is 3.99.

In addition, we also find some hyper-conjugative bonding for HNO and NOH. In HNO, the weak bond orders between Oℓ2 and Nh (0.27) and between Oℓ2 and H (−0.27) manifestly have the same implications as the similar weak bond orders of Oℓ2* we found in FOOH: they indicate weak dative bonding between the lone pair Oℓ2 and the antibonding orbital in the NH bond. An analogous, though somewhat weaker dative bonding is indicated in NOH by the bond orders between Nℓ2 and Oh (0.12) and between Nℓ2 and H (−0.12).

At the transition state, the situation is different. If one diagonalizes here the 3 × 3 density submatrix between the quasi-atomic orbitals Nh, Oh, and H, then one obtains a result similar to what is well known for triangular three-center, three-orbital, four electron systems. Table 8 lists the expansions of these "local natural orbitals" in terms of the quasi-atomic orbitals Nh, Oh, H and their occupation numbers. Nearly two electrons are seen to occupy a nodeless three-center bond orbital and nearly two electrons occupy an orbital with *one* node that separates Oh from Nh and H and manifestly runs close to H, which has a small contribution. The third orbital, with *two* nodes is correlating and has an occupation of only 0.04. The reasons for the weakened bond orders in the bonds H–Nh (0.58) and H–Oh (0.78) as well as the antibonding bond order (−0.42) between Nh and Oh of Table 6 are manifest from Table 8: two electron have to occupy an orbital with considerable antibonding character. This accounts for the energy barrier of 117 millihartree with respect to HNO.

The "local split-localized" description is obtained by localizing the two nearly doubly occupied local natural orbitals. This results in an (Nh–H)-bonding orbital and an (Oh–H)-bonding orbital. The expansions of the resulting orbitals in terms of the quasi-atomic orbitals Nh, H, Oh are listed in Table 9 and the bond order matrix between them, which is still nearly diagonal, is shown in Table 10. The Oh–H bond orbital is manifestly quite covalent and contributes a bond order of 0.96 to the OH bond. The Nh–H bond orbital, on the other hand, is quite polarized towards nitrogen and only weakly covalent, with a node separating Oh from H and Nh, orthogonalizing it to the Oh–H bond orbital. The Nh–H orbital contributes a bond order of only 0.52 to the N–H bond, a bond order of −0.17 to the O–H bond, and a bond order of −0.52 to the N-H bond. It can be considered as a nitrogen lone-pair that is forced into close proximity of the Oh–H bonding orbital. In this orbital representation, the destabilization of the transition state is thus a result of the *non-bonded*

Table 5 Density matrix for HNO after localization and after orientation

QAO	*H*	Nℓ1	Nh	Noσ	Noπ	Oℓ1	Oℓ2	On π	On σ
H	**1.05**		**0.93**				−0.27		−0.08
Nℓ		**1.99**							
Nh	**0.93**		**1.03**	0.09			0.27		
Noσ			0.09	**0.94**					**0.96**
Noπ					**0.91**			**0.90**	
Oℓ1						**2.00**			
Oℓ2	−0.27		0.27				**1.91**		−0.03
Onπ					**0.90**			**1.10**	
Onσ	−0.08			**0.96**			−0.03		**1.06**

Table 6 Density matrix for NHO* after localization and after orientation

QAO	Nℓ1	Nh	Noσ	Noπ	H	Oℓ1	Oh	Onπ	Onσ
Nℓ1	**1.99**		0.01						
Nh		**1.65**	−0.07		**0.58**		**−0.42**		0.01
Noσ	0.01	−0.07	**0.91**		0.07		0.02		**0.94**
Noπ				**0.74**				**0.87**	
H		**0.58**	0.07		**0.95**		**0.78**		0.04
Oℓ1						**2.00**			
Oh		**−0.42**	0.02		**0.78**		**1.39**		−0.09
Onπ				**0.87**				**1.27**	
Onσ		0.01	**0.94**		0.04		−0.09		**1.10**

Table 7 Density matrix for NOH after localization and after orientation

QAO	Nℓ1	Nℓ2	Noσ	Noπ	Oℓ1	Onπ	Onσ	Oh	H
Nℓ1	**1.99**								
Nℓ2		**1.98**						0.12	−0.12
Noσ			**0.92**				**0.96**		−0.06
Noπ				**0.69**		**0.90**			
Oℓ					**2.00**				
Onπ				**0.90**		**1.31**			
Onσ			**0.96**				**1.08**	0.06	
Oh		0.12					0.06	**1.05**	**0.96**
H		−0.12	−0.06					**0.96**	**0.96**

repulsions between the two doubly filled orthogonally interpenetrating orbitals.

The total atomic valence electron populations for hydrogen, nitrogen and oxygen respectively changes from 1.05, 4.87, 6.08 in HNO to 0.95, 5.29, 5.76 in NHO*, and then to 0.96, 5.58, 5.44 in NOH. This shift of charge from oxygen to nitrogen is manifestly required by the hydrogen bond rearrangement and is the reason for HNO being more stable than NOH.

4 Three-center bonding in $H_2BH_2BH_2$

Longuet-Higgins [12] originally proposed that the stability of boron hydrides is the result of energetically favorable three-center B–H_b–B (b = bridging) two-electron bonds. Lipscomb [13] confirmed the geometric as well as the electronic structures, the former by X-ray crystallography, the latter by means of localized SCF orbitals. The simplest boron hydride, $H_2BH_2BH_2$, contains two such three-center

Table 8 Natural orbitals among the three reactive quasi-atomic orbitals Nh, H, Oh at the NHO* transition state

Natural orbital type	N–H–O bonding	N–O antibonding	N–H and O–H antibonding
Occupation no.	1.992	1.956	0.044
Coefficient of Nh	0.621	0.669	−0.407
Coefficient of H	0.661	0.169	0.731
Coefficient of Oh	0.420	−0.723	−0.548

Table 9 Three-center split-localized molecular orbitals at the NHO* transition state in terms of quasi-atomic orbitals

	Nh–H bond	Oh–H bond	Oh–H–Nh–Corr
Nh	0.912	0.056	−0.407
H	0.288	0.619	0.731
Oh	−0.293	0.784	−0.548

Table 10 Density matrix for the three-center split-localized molecular orbitals at the NHO* transition state

	Nh–H bond	Oh–H bond	Oh–H–Nh–Corr
Nh–H bond	1.977	0.017	0
Oh–H bond	0.017	1.970	0
Oh–H–Nh–Corr	0	0	0.044

bridging bonds and it offers the opportunity to test whether three center bonds will intrinsically emerge from and be successfully described by our approach.

We chose the experimental geometry determined by Duncan and Harper [14], given by the following parameters of the D_{2h} structure (t = terminal, b = bridging): $r_{BB} = 1.743$ Å, $r_{BHt} = 1.184$ Å, $r_{BHb} = 1.314$ Å, $\angle_{HtBHt} = 121.5°$. The FORS wavefunction of the A_g ground state consists of 1,129,033 A_g determinants. We obtained the SCF energy −52.83247 and the FORS energy −52.95136.

The oriented quasi-atomic orbitals are exhibited in Fig. 3 and present a very simple picture: each boron atom has four quasi-atomic orbitals, each one pointing to one of its four hydrogen neighbors, each of which has a quasi-atomic molecular orbital associated with it. There are no lone pairs in this molecule.

The first-order density matrix expressed in terms of the oriented quasi-atomic orbitals is shown in Table 11. Elements that are less than 0.01 have been omitted. The large elements, which are printed in bold face in the table, are also entered in the figure at the appropriate places.

While each of the four end hydrogen atoms carries a charge of 1.03, each central bridging hydrogen has a charge of 0.78. The total charge on each boron atom is 3.15. There is thus a strong charge shift away from the central hydrogen atoms.

The largest bond orders (0.96) occur for the end bonds between the orbitals Btx and Htx ($x = 1, 2, 1^*, 2^*$).

The central bridging hydrogen orbital Hc1 is bonded to the orbital Bc1 on one boron as well as to the orbital Bc1* on the other boron, in both cases with the bond order 0.66. In addition, a strong bond order (0.57) also exists directly between the boron quasi-atomic orbitals Bc1, Bc1* pointing to the same central hydrogen. A central three-center bond emerges thus from this part of the density matrix. Diagonalization of the density submatrix between these three quasi-atomic MOs will undoubtedly yield a three-center bonding orbital with an occupation not much less than 2, a left-right-antisymmtric correlating orbital, containing no hydrogen contributions, with a relatively low occupation, and a practically empty orbital with two nodes.

Exactly the same bonding pattern emerges from the density matrix elements between the orbitals Hc2, Bc2 and Bc2*, which therefore also form a three-center bond. Note, however, that *all bond orders between the orbital set Bc1, Bc1*, Hc1 and the orbital set Bc2, Bc2*, Hc2 are very small*. Thus, we have indeed two three-center bonds and, in spite of the closeness of these two bonds, not a four-electron six-center bond.

We also note that all large bond orders are close to the maximum value compatible with the given occupations, as discussed in Sect. 8 of the preceding paper.

5 Hyperconjugation in H_2CO

Formaldehyde is generally described as containing a C–O double bond in which the charge is polarized toward the oxygen. The remaining valence electrons are considered to occupy two non-interacting oxygen lone pairs and two C–H bonding orbitals. Textbooks often go further to say that the resonance structure in which there are three lone pairs on the oxygen atom is a non-negligible contributor to the overall electronic structure. It is therefore of interest to see what an unbiased intrinsic analysis of the unbiased full-valence-space MCSCF wavefunction of 11,148 determinants will reveal regarding bonding and non-bonding orbitals in this system.

We use the experimental geometry of Yamada et al. [15] which has the following parameters: $r_{CO} = 1.203$ Å, $r_{CH} = 1.099$, $\angle_{HCH} = 116.5°$. The FORS wavefunction for the ground state has 11,148 determinants of A_1 symmetry. We obtained the SCF energy −113.90844 and the FORS energy −114.04183 hartree.

The oriented quasi-atomic orbitals are displayed in Fig. 4. For each of the two C–H bonds as well as for the sigma and pi bonds between carbon and oxygen the appropriate quasi-atomic orbitals are generated. There are two lone pair orbitals on oxygen, one a distorted 2s-type, the other a 2pπ-type in the molecular plane.

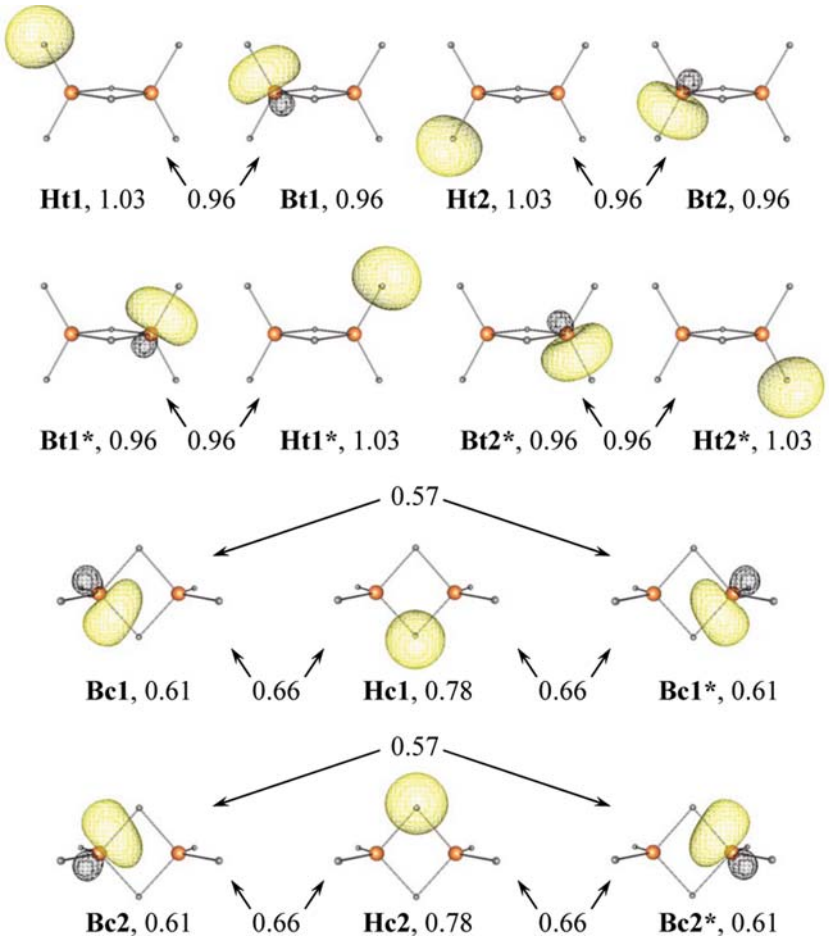

Fig. 3 Oriented quasi-atomic orbitals for B_2H_6. Occupation numbers are given next to the orbital labels and large bond orders are indicated between *arrows* pointing to the orbitals involved

Table 11 Density matrix for B_2H_6 after localization and after orientation

QAO	Ht1	Ht2	Bt1	Bt2	Bc1	Bc2	Hc1	Hc2	Bc1*	Bc2*	Bt1*	Bt2*	Ht1*	Ht2*
Ht1	**1.03**	−0.08	**0.96**				−0.02	−0.02	−0.09	−0.09			−0.03	0.08
Ht2	−0.08	**1.03**		**0.96**			−0.02	−0.02	−0.09	−0.09			0.08	−0.03
Bt1	**0.96**		**0.96**	0.08	0.08	0.08	0.04	0.04	−0.02	−0.02	0.05	−0.06		
Bt2		**0.96**	0.08	**0.96**	0.08	0.08	0.04	0.04	−0.02	−0.02	−0.06	0.05		
Bc1			0.08	0.08	**0.61**	0.08	**0.66**	−0.03	**0.57**	0.06	−0.02	−0.02	−0.09	0.09
Bc2			0.08	0.08	0.08	**0.61**	−0.03	**0.66**	0.06	**0.57**	−0.02	−0.02	−0.09	−0.09
Hc1	−0.02	−0.02	0.04	0.04	**0.66**	−0.03	**0.78**	−0.15	**0.66**	−0.03	0.04	0.04	−0.02	−0.02
Hc2	−0.02	−0.02	0.04	0.04	−0.03	**0.66**	−0.15	**0.78**	−0.03	**0.66**	0.04	0.04	−0.02	−0.02
Bc1*	−0.09	−0.09	−0.02	−0.02	**0.57**	0.06	**0.66**	−0.03	**0.61**	0.08	0.08	0.08		
Bc2*	−0.09	−0.09	−0.02	−0.02	0.06	**0.57**	−0.03	**0.66**	0.08	**0.61**	0.08	0.08		
Bt1*			0.05	−0.06	−0.02	−0.02	0.04	0.04	0.08	0.08	**0.96**	0.08	**0.96**	
Bt2*			−0.06	0.05	−0.02	−0.02	0.04	0.04	0.08	0.08	0.08	**0.96**		**0.96**
Ht1*	−0.03	0.08			−0.09	−0.09	−0.02	−0.02			**0.96**		**1.03**	−0.08
Ht2*	0.08	−0.03			−0.09	−0.09	−0.02	−0.02				**0.96**	−0.08	**1.03**

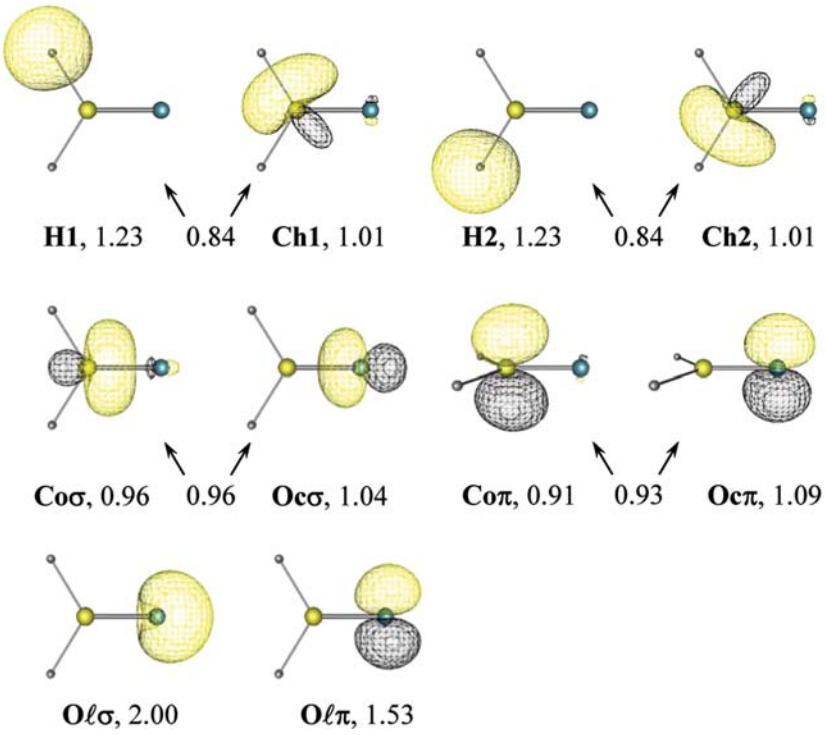

Fig. 4 Oriented quasi-atomic orbitals for H_2CO. Occupation numbers are given next to the orbital labels and large bond orders are indicated between *arrows* pointing to the orbitals involved

The density matrix for the oriented localized orbitals is given in Table 12. Bond orders of less than 0.01 are not shown. The large elements, populations as well as major bond orders, are printed in bold face in the table and also entered in the figure at the appropriate places. The orientation procedure clearly reveals the two carbon-hydrogen bonds and the sigma and pi bonds between carbon and oxygen.

The total valence electronic populations of hydrogen, carbon and oxygen are 1.23, 3.88, and 5.66, respectively.

There are, however, additional non-negligible bond orders between the oxygen lone pair orbital O$\ell\pi$ and the hydrogen orbitals as well as the carbon orbitals pointing to the hydrogens. This appears to imply slight additional pi bonding between oxygen and carbon as well as small anti-bonding interactions between oxygen and each of the hydrogen atoms. These interactions are consistent with the O$\ell\pi$ orbital having an occupation of only 1.53 electrons, which is markedly less than is typically found for a lone pair. The origin of these weak interactions can again be understood by taking a look at local split-localized orbitals.

We replace the two hydrogen orbitals with their orthonormalized plus and minus combinations and, similarly, the carbon orbitals Ch1 and Ch2 by their plus and minus combinations Chσ and Chπ. The first two rows of Fig. 5 display these four orbitals together with the O$\ell\pi$ orbital. The figure also shows all populations and bond-orders of this transformed orbital set. It is apparent that the Chπ orbital is mainly bonded to the H1–H2 orbital but also somewhat

Table 12 Density matrix for H_2CO after localization and after orientation

QAO	H1	H2	Ch1	Ch2	Coσ	Coπ	O$\ell\sigma$	O$\ell\pi$	Ocπ	Ocσ
H1	**1.23**	−0.28	**0.84**	0.13				**−0.33**		−0.13
H2	−0.28	**1.23**	0.13	**0.84**				**0.33**		−0.13
Ch1	**0.84**	0.13	**1.01**	0.05	0.13			**0.48**		
Ch2	0.13	**0.84**	0.05	**1.01**	0.13			**−0.48**		
Coσ			0.13	0.13	**0.96**	0.02				**0.96**
Coπ					0.02	**0.91**			**0.93**	
O$\ell\sigma$							**2.00**			
O$\ell\pi$	**−0.33**	**0.33**	**0.48**	**−0.48**				**1.53**		
Ocπ						**0.93**			**1.09**	−0.01
Ocσ	−0.13	−0.13			**0.96**				−0.01	**1.04**

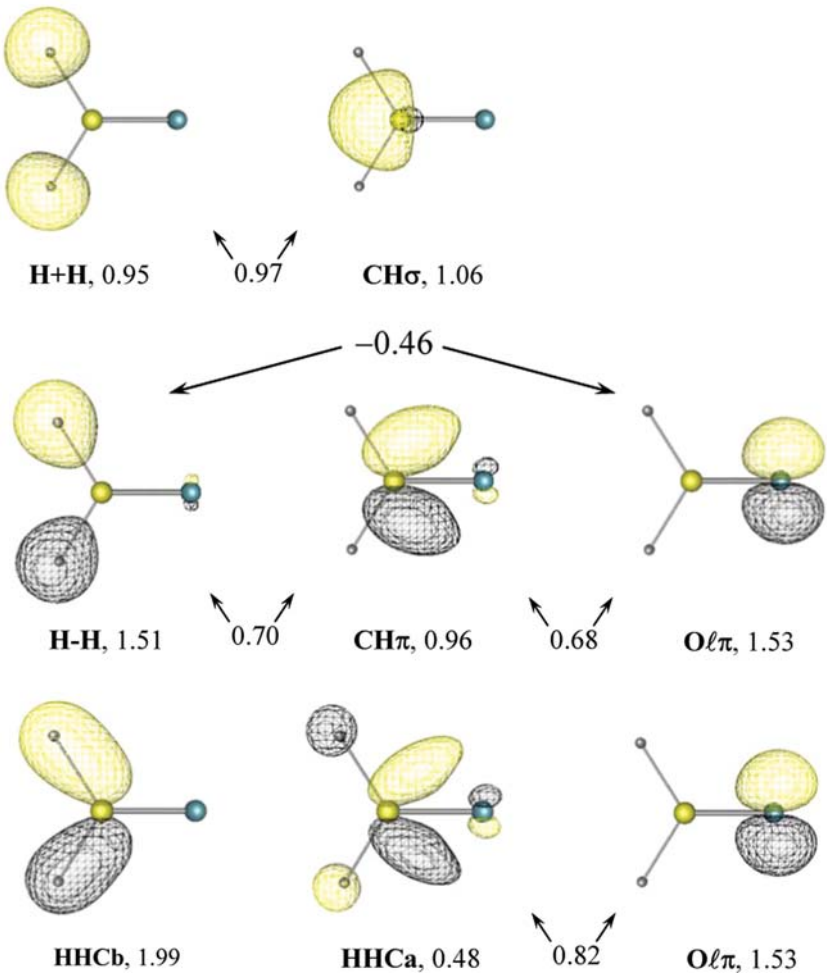

Fig. 5 *Top row* orthonormalized plus (symmetric) combinations of the two hydrogen orbitals and of the corresponding interacting carbon orbitals. *Middle row* orthonormalized minus (antisymmetric) combinations of the two hydrogen orbitals and of the corresponding interacting carbon orbitals together with the oxygen lone pair orbital O$\ell\pi$. *Bottom row* the bonding and anti-bonding orbitals formed from the antisymmetric (H-H) and CHπ orbitals of the middle row together with the oxygen lone pair orbital O$\ell\pi$. Occupation numbers are given next to the orbital labels and bond orders are indicated between *arrows* pointing to the orbitals involved

to the oxygen lone pair orbital O$\ell\pi$, which in turn has an anti-bonding interaction with the H1–H2 orbital.

In order to understand this anti-bonding, we now diagonalize the 2 × 2 density matrix between Chπ and H1–H2, which yields, from them, a bonding combination orbital HHCb and an antibonding combination orbital HHCa. In the last row of Fig. 5, these two orbitals are displayed together with the oxygen lone pair orbital O$\ell\pi$, and all populations and bond-orders of this transformed orbital set are entered. Note that HHCB is polarized towards the hydrogens whereas HCCa is polarized toward carbon. The bonding orbital HHCb has an occupation of 1.99 and can therefore not interact with another orbital. The bond order between HHCb and O$\ell\pi$ is in fact 0.003.

On the other hand, the anti-bonding orbital HCCa has a substantial correlating occupation of 0.48 and the oxygen lone pair O$\ell\pi$has only an occupation of 1.53. According to Sect. 8 of the preceding paper, this allows for a maximum bond order of 0.85 between these two orbitals. The actual bond order, shown in Fig. 5, of 0.82 is close to that. The corresponding energy lowering results from the positive overlap between the oxygen lone pair O$\ell\pi$and the carbon end of the HHCa orbital, but it necessarily entails a negative overlap between the oxygen lone pair and the hydrogen end of the HHCa orbital. However, the interatomic energy integrals between the oxygen orbitals and the hydrogen orbitals are obviously much weaker than those between the oxygen orbitals and the carbon orbitals. In summary, there is a tendency to make a third carbon to oxygen bond but, since it has to go via the carbon to hydrogen anti-bonding orbital, it remains weak. As was also noted in the case of FOOH, this type of hyper-conjugation results therefore from a partial bond formation between oxygen and carbon *combined with a correlation stabilization between carbon and the two hydrogens*.

6 Conclusions

The ILDA method, based on oriented quasi-atomic orbitals, proves to be a useful uncomplicated tool for extracting information on the electronic structure that is embedded in the most general optimal MCSCF wavefunction in a full valence

space. The bonding patterns in each system are clearly exhibited in considerable detail. Notable is the marked separation that can be achieved between the various bonding regions in a molecule, for instance between the two three-centers bonds in diborane, which are clearly brought to light, or between the reaction and the spectator orbitals in the HNO isomerization, which yields a transparent structure of the transition state.

Finer features of bonding patterns can be uncovered by analyzing the local natural and the local split-localized orbitals in terms of the quasi-atomic orbitals. The combined use of these transformation-related orbitals proves an effective tool for elucidating bonding interactions. This is exemplified by the discussion of the NHO transition state and by the identification of hyperconjugative effects in several molecules. As regards the latter, the analysis reveals that hyperconjugation is contingent on the presence of antibonding orbitals that *provide sufficiently large electron correlation for the corresponding bonding orbitals*.

Since full-valence space MCSCF wavefunctions are the best that can be constructed from M (= total *number* of minimal basis set orbitals in the molecule) molecular orbitals, and since all elements of the foregoing analysis are unbiased, intrinsic and basis set independent, the deduced inferences supersede that of any other type of wavefunction generated from this many or a lesser number of orbitals. The *method* of analysis manifestly does not depend on the basis set size and, in principle, one should determine the complete basis set limit of the results. It seems however unlikely that proceeding from a triple-zeta to a quadruple-zeta AO or higher basis would introduce qualitative changes, although this surmise should be checked.

It is apparent that each determinant constructed from the quasi-atomic orbitals (or from their bonding and antibonding combinations) will have valence-bond-like character.

Writing a wavefunction in terms of these determinants [16] will therefore generate its appropriate VB interpretation as had already been illustrated in the third paper of Reference [5].

Acknowledgments The authors thank Dr. Michael W. Schmidt for his helpful advice and for performing some of the calculations at the transition state NHO* in Sect 3. The present work was supported by the Division of Chemical Sciences, Office of Basic Energy Sciences, U.S. Department of Energy under Contract No. W-7405-Eng-82 with Iowa State University through the Ames Laboratory.

References

1. Ivanic J, Atchity G, Ruedenberg K J Chem Phys (preceding paper)
2. Ruedenberg K, Sundberg KR (1976) In: Calais J-L, Goscinski O, Linderberg J, Öhrn Y (eds) Quantum Science. Plenum Press, New York, p. 505
3. Cheung LM, Sundberg KR, Ruedenberg K (1978) J Am Chem Soc 100:8024
4. Cheung LM, Sundberg KR, Ruedenberg K (1979) Int J Quantum Chem 16:1103
5. Ruedenberg K, Schmidt MW, Gilbert MM, Elbert ST (1982) Chem Phys 71:41, 51, 65
6. Dunning THJr (1989) J Chem Phys 90:1007
7. Ivanic J, Ruedenberg K (2001) Theor Chem Acc 106:339
8. Chaban G, Schmidt MW, Gordon MS (1997) Theor Chem Acc 97:88
9. Schmidt MW, Baldridge KK, Boatz JA, Elbert ST, Gordon MS, Jensen JH, Koseki S, Matsunaga N, Nguyen KA, Su SJ, Windus TL, Dupuis M, Montgomery JA (1993) J Comput Chem 14:1347. http://www.msg.ameslab.gov/GAMESS/GAMESS.html
10. Lee TJ, Rice JE, Datos CE (1996) Mol Phys 89:1359
11. Dalby FW (1958) Can J Phys 36:1336
12. Longuet-Higgins HC (1949) J Chem Phys 46:268
13. Lipscomb WN (1977) Science 196:1047
14. Duncan JL, Harper J (1984) Mol Phys 51:371
15. Yamada K, Nakagawa T, Kuchitsu K, Morin Y (1971) J Mol Spectrosc 38:70
16. Atchity GJ, Ruedenberg K (1999) Have discussed methods for performing such wave function transformations. J Chem Phys 111:2910